Bacteriochlorophyll in Electric Field

Pär Kjellberg, Zhi He, and Tõnu Pullerits*

Department of Chemical Physics, Lund University, P.O. Box 124, S-22100 Lund, Sweden

Received: June 10, 2003; In Final Form: October 8, 2003

The spectroscopic properties of a molecule is strongly dependent on interactions with the surrounding environment. We have used time dependent density functional theory (TDDFT) and a multilevel perturbation model to study the transition energies, polarizability, and dipole moments of a bacteriochlorophyll in an electric field. The perturbation Hamiltonian was constructed as to give an electric field dependence of the transition energies in agreement with the result from TDDFT. It was found that, to reach agreement, it was not enough to use the Q and Soret bands of the bacteriochlorophyll; additional energy levels had to be introduced. The change in dipole moment and polarizability for the two lowest excited states Q_x and Q_y were calculated. Our calculations predict a negative change in polarizability $\Delta\alpha$ for the ground state to Q_y transition.

1. Introduction

Primary processes of photosynthesis are light absorption and excitation transfer in antenna, followed by electron transfer in the reaction center. The initial stage of light harvesting is highly optimized.[1−4] This is achieved by making the elementary transfer steps extremely fast and forming an energy funnel around the reaction center. Another property that contribute to effectiveness is the excellent light collection obtained by the large absorption cross section. To maximize the cross section the light-harvesting antennas are built up from various pigment molecules complementing each other by absorbing in different wavelength regions. For example in the light harvesting systems of photosynthetic bacteria, one usually finds two types of pigment molecules: bacteriochlorophylls (BChl) and carotenoids (Car). It is not only the chemical identity of the pigment molecule but also the local environment which is of importance in determining the absorption spectra of the molecule. The same types of molecules can have different properties depending on interactions with nearby molecules.

The influence of the local environment on the absorption of a pigment molecule is well illustrated by the BChl in various antennas. A monomeric BChl in pyridine solution has absorption maximum of the Q_y transition at around 780 nm. Peripheral light harvesting antenna (LH2) of purple bacteria contains two rings of BChl molecules[6,7] B800 and B850, named according to the wavelengths of their characteristic Q_y transition (800 and 850 nm respectively). In the B800 ring the intermolecular distances are about 20 Å this is large enough for the BChls to be considered monomeric. The B850 ring, on the other hand, is a densely packed system with significant excitonic effects[9−15] lowering the energy of the main band of BChl absorption. A subunit of a core antenna (LH1) of purple bacteria, a dimer of BChl, absorbs at 820 nm whereas the intact LH1 has absorption maximum at around 880 nm. A strongly coupled BChl dimer in the reaction center, a so-called special pair, absorbs even further toward the red. Part of the variation in absorption wavelength can be explained by intermolecular excitonic couplings, however the details of the protein binding pocket with specific interactions like hydrogen bonding and axial ligation play a crucial role. It has also been suggested that the rotation of the BChl acetyl group can lead to large spectral shifts.[16,17] However, in the assignment of the transition energies of BChl molecules in a so-called FMO complex,[8] no obvious correlation between the energies and the acetyl group orientations can be identified.

Site-directed mutagenesis breaking up hydrogen bonds between the B850 BChl of *Rhodobacter (Rb.) sphaeroides* and nearby amino acids, shifts the Q_y band from 850 to 838 or 826 nm, for one and two broken hydrogen bonds respectively.[18,19] Similar effects has been demonstrated with B800.[20] In this context it is remarkable that the B800 binding sites in two different purple bacteria with resolved structure, *Rhodopseudomonas (Rps.) acidophila* and *Rhodospirillum (Rs.) molischianum*, are very different. In *Rps. acidophila* there are two hydrogen bonds between B800 acetyl carbonyl and the $\beta Arg20$ amino acid, whereas there are no known hydrogen bonds in *Rs. molischianum*. The axial ligands of B800 in these two LH2s are also different. In *Rps. acidophila* the central magnesium is ligated by a formyl methionine $\alpha fMet_1$, whereas in *Rs. molischianum*, it is ligated by a negatively charged residue aspartate (αAsp_6). DFT studies where the hydrogen bonding residues and axial ligands were included in the calculations showed that these differences to a large extent cancel each other out, leading to very similar Q_y transition energies.[22] Recently the calculations for *Rps. acidophila* were repeated with the above two amino acids replaced by corresponding atomic point charges.[21] Comparison of these two calculations indicates that for the hydrogen-bonding residue the model of point charges gives significantly smaller red-shift compared to the full calculation where the amino acid is explicitly included. On the other hand, the ultrafast carotenoid band-shift detected upon BChl excitation in LH2[23] were well explained via changes of the local fields due to different atomic point charges in BChl ground and excited states.[24]

Besides systematic differences of BChl binding sites which lead to different spectral bands in BChl-protein complexes, there are always slow random fluctuations of the local environment and of the BChl configuration, leading to inhomogeneous spectral broadening.[25,26] Recently it was argued that part of the inhomogeneous broadening of the B800 line in the LH2 spectrum can be attributed to the influence of local electric fields on the BChl molecules.[27] It was shown that, using a simple

10.1021/jp035642y CCC: $25.00
Published on Web 11/15/2003

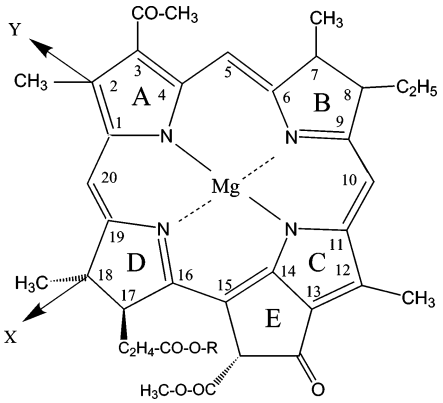

Figure 1. Molecular structure of bacteriochlorophyll and definition of the molecular axis. R = phytyl.

two-level energy scheme, the asymmetric shape of B800 absorption band, usually explained in terms of phonon wing and/or higher energy weakly allowed B850 exciton bands,[35] can be reproduced by assuming Gaussian distribution of the local electric field.

Experimentally the field-induced spectral changes are usually studied by Stark spectroscopy.[28−30] In this method, the broadening and shift of the spectral band, induced by an external electric field, is observed. The line broadening and shift are related to the difference in the electrical dipole moment ($\Delta\mu$) and polarizability ($\Delta\alpha$), respectively. In analysis the local field due to the environment has to be taken into account. Generally the local fields are unknown and can be (and usually are) larger than the externally applied fields in different field-sensitive experiments.

Computationally various quantum chemistry methods can be used to study the effects of the electric field on molecular properties. For example, Grozema et al.[31] used time dependent density functional theory (TDDFT) to study the excited state polarizabilities of conjugated molecules. They found a good agreement between calculated and experimentally measured $\Delta\alpha$.

In the current work, we have performed a computational study of the properties of BChl in electric field. The effect of an electric field on the two lowest lying excited states in the BChl is calculated by TDDFT. The result is analyzed in terms of changes of the electrical dipole and polarizability upon excitation; see section 2. A minimum multilevel perturbation model of the BChl was constructed using experimentally established transition energies and transition dipole moments. Using the information from TDDFT about the change in dipole moment and including additional states, a multilevel scheme was foundconstructed giving a satisfactory fit to the TDDFT results, section 3.

2. TDDFT

The effect of electrostatic fields on the Q bands of the BChl molecule was studied using time-dependent density functional theory with the three-parameter Lee−Yang−Parr (B3LYP) functional.[32] The calculations were performed with the Gaussian 98 program package,[33] with a 6-31G basis set. We used the coordinates of the B800 BChl molecule in crystal structure of *Rps. acidophilla* (strain 10050) reported by McDermott et al.[6] The hydrogen positions were generated by geometry optimization at Hartree−Fock level.

The *X* and *Y* axes of the BChl are defined as the N(B)−N(D) and N(C)−N(A) directions, respectively (see Figure 1). The *Z* axis is perpendicular to the *XY* plane. A series of TDDFT calculations were carried out with electric fields ranging from −50 to +50 MV/cm oriented in the *X*, *Y*, and *Z* direction. To check the sufficiency of the basis set the calculations were repeated for two of the field strengths with the more extended split valence with polarization (SVP) basis. The result of the calculations are summarized in Tables 1 and 2.

We are aware of two estimates of BChl Q_y and Q_x transition energies in vacuum, both based on the solvent shifts of the corresponding bands: 13 341 and 17 660 cm^{-1} by Renge et al.[36] and 13 590 and 18 150 cm^{-1} by Limantara et al.[37] Compared to this TDDFT gives higher values for the transition energies: 15 275 and 19 123 cm^{-1} with the 6-31G basis and 14 943 and 18 739 cm^{-1} with the SVP basis. It is often the case that quantum chemical methods overestimate the energies for large systems. In principle, TDDFT is an exact reformulation of the many-body Schrödinger equation. However one does not know the exact exchange correlation functional. The B3LYP used here is a semiempirical functional not tuned to all kinds of systems.

To make comparison with experiment sometimes the energies are systematically scaled.[38] In the current work the calculated energies of the Q_y and Q_x transitions at zero electric field have been shifted as to coincide with the experimental BChl absorption maxima in solution.[34] The result from the calculations with field was adjusted by the same energy, 2488 and 2757 cm^{-1} for the Q_y and Q_x transitions respectively (2373 and 2156 cm^{-1} when using the SVP basis).

The adjusted transition energies for fields in the *X* and *Y* directions varying from −50 to +50 MV/cm are presented in Figure 2. As can be seen from the figure, the electric field effect on the transition energies is very much the same for the two different basis sets.

TABLE 1: Comparison of Calculated B800 Q_y Transition in the Different Charge Fields[a]

	$Q_y(X)$			$Q_y(Y)$			$Q_y(Z)$		
fields (MV/cm)	cm^{-1}	f[b]	P[c] (deg)	cm^{-1}	f	P (deg)	cm^{-1}	f	P (deg)
				6-31G Basis					
−50	14 857	0.3443	1.2	15 796	0.3496	4.1			
−25	15 143	0.3615	1.8	15 428	0.3605	3.3	15 245	0.3650	2.6
−12.5	15 226	0.3652	2.1	15 326	0.3642	2.9	15 261	0.3658	2.6
0	15 275	0.3661		15 275	0.3661		15 275	0.3661	
12.5	15 292	0.3644	3.1	15 272	0.3660	2.2	15 286	0.3663	2.6
25	15 279	0.3601	3.7	15 318	0.3640	1.8	15 295	0.3664	2.6
50	15 153	0.3435	4.1	15 553	0.3532	0.5			
				SVP Basis					
−25	14 818	0.3592		15 092	0.3576				
0	14 943	0.3638		14 943	0.3638				

[a] The notation (*X*) (or (*Y*), (*Z*)) indicates that the field is along the *X* (or *Y*, *Z*) axis of the B800 BChl displayed in Figure 1. [b] *f* oscillator strengths. [c] Polarization in degrees, which refers to the angles of transition dipole moments with respect to the *Y* axis of the B800 BChl.

TABLE 2: Comparison of Calculated B800 Q_x Transition in the Different Charge Fields

	$Q_x(X)$			$Q_x(Y)$			$Q_x(Z)$		
fields (MV/cm)	cm^{-1}	f [b]	P [c] (deg)	cm^{-1}	f	P (deg)	cm^{-1}	f	P (deg)
				6-31G Basis					
−50	18 925	0.0296	82.3	18 908	0.0529	90.9			
25	19 056	0.0447	95.1	19 195	0.0397	90.4	19 173	0.0498	92.9
12.5	19 093	0.0488	94.1	19 125	0.0498	92.3	19 149	0.0503	93.1
0	19 123	0.0507	87.2	19 123	0.0507	87.2	19 123	0.0507	87.2
12.5	19 145	0.0504	92.4	19 071	0.0534	94.4	19 095	0.0511	93.1
25	19 158	0.0470	92.1	18 965	0.0581	96.5	19 068	0.0514	93.2
50	19 096	0.0355	92.3	18 539	0.0757	102.4			
				SVP Basis					
−25	18 666	0.0372		18 841	0.0357				
0	18 739	0.0426		18 739	0.0426				

[a] The notation (*X*) (or (*Y*), (*Z*)) indicates that the field is along the *X* (or *Y*, *Z*) axis of the B800 BChl displayed in Figure 1. [b] *f* oscillator strengths. [c] Polarization in degrees, which refers to the angles of transition dipole moments with respect to the *Y* axis of the B800 BChl.

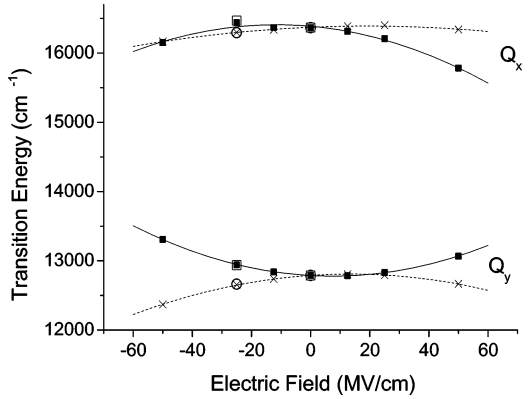

Figure 2. TDDFT calculated gs → Q_y and gs → Q_x transition energies as a function of the electric field: crosses (6.31G) and circles (SVP) calculated with the field in *X* direction; filled (6.31G) and unfilled (SVP) squares with the field in *Y* direction. The lines are fits to eq 1.

TABLE 3: Dipole and Polarizability Changes as Obtained from the TDDFT Calculations

state	dir	$\Delta\mu$ (D)	$\Delta\alpha$ (Å^3)
Q_y	*X*	−0.173	3.87
	Y	0.141	−5.73
	Z	−0.0592	0.260
Q_x	*X*	−0.107	1.67
	Y	0.226	5.89
	Z	0.125	0.129

The transition energy dependence on the electric field **F** can be expressed as:[31]

$$E_{\mathrm{exc}}(\mathbf{F}) = E_{\mathrm{exc}}(0) - \Delta\boldsymbol{\mu}\mathbf{F} - \frac{1}{2}\Delta\alpha\mathbf{F}^2 \qquad (1)$$

where $E_{\mathrm{exc}}(0)$ is the excitation energy at zero field, $\Delta\boldsymbol{\mu}$ is the change in dipole moment, and $\Delta\alpha$ is the change in polarizability. Higher order terms have been neglected here. From this equation it is easy to see that since the energy is linearly dependent on the change in dipole during excitation, the effect will not be the same for positive and negative fields, leading to an asymmetric dependence. The change in dipole moment and polarizability were obtained by fitting the TDDFT calculations to eq 2. The results are presented in Table 3 and Figure 2.

3. Multilevel Model of BChl

Static electric field applied to a molecule perturbs the Hamiltonian. In dipole approximation the perturbation energy can be expressed as the scalar product of the dipole moment $\boldsymbol{\mu}$ and the electric field **F**:

$$H' = -\boldsymbol{\mu}\mathbf{F} \qquad (2)$$

Following the model proposed by van Mourik et al.,[27] we can express the perturbed molecular Hamiltonian for a $N+1$ level system whith index zero for the ground state as

$$H = \begin{bmatrix} \nu_0 - \boldsymbol{\mu}_{00}\mathbf{F} & -\boldsymbol{\mu}_{01}\mathbf{F} & \cdots & -\boldsymbol{\mu}_{0N}\mathbf{F} \\ -\boldsymbol{\mu}_{10}\mathbf{F} & \nu_1 - \boldsymbol{\mu}_{11}\mathbf{F} & \cdots & -\boldsymbol{\mu}_{1N}\mathbf{F} \\ \vdots & & \ddots & \\ -\boldsymbol{\mu}_{N0}\mathbf{F} & & \cdots & \nu_N - \boldsymbol{\mu}_{NN}\mathbf{F} \end{bmatrix} \qquad (3)$$

Here ν_i are the unperturbed eigenenergies of the system and the electric field couples to the dipole moments $\boldsymbol{\mu}_{ij} = -e\langle i|\mathbf{q}|\, j\rangle$, **q** is the electron coordinate operator, and *e* is the electric charge of an electron. Diagonalization of the Hamiltonian gives the eigenenergies of the system in the field.

The dipoles of the system in the field can be calculated from the eigenvectors of the Hamiltonian as

$$\boldsymbol{\mu}_{\phi\varphi} = -e\langle\phi|\mathbf{q}|\varphi\rangle = \sum_{ij}^{N} \phi_i\varphi_j^*\mu_{ij} \qquad (4)$$

where $\boldsymbol{\mu}_{\phi\varphi}$ is the new dipole and $\langle\phi|$ and $|\varphi\rangle$ are the new states given by the eigenvectors

$$|\varphi\rangle = \sum_{i}^{N} \varphi_i|i\rangle \qquad (5)$$

and

$$\langle\phi| = \sum_{j}^{N} \phi_j^*\langle j| \qquad (6)$$

The *N*-level Hamiltonian in eq 3 leads to *N*th power dependence of the state energies on the field. Thereby, for $N > 2$, hyperpolarizabilities also are included in the description. The Hamiltonian (eq 3) can be used to derive the quantum mechanical second-order perturbative sum over states expression of the polarizabilities

$$\alpha_n = \frac{2}{3}\sum_{i=0,i\neq n}^{N} \frac{|\boldsymbol{\mu}_{in}|^2}{\nu_i - \nu_n} \qquad (7)$$

The higher order expansions lead to corresponding expressions for hyperpolarizabilities.

We constructed a minimal multilevel model of the BChl which reasonably well reproduced the TDDFT calculations and did not contradict experimental results. We started with electronic states and corresponding transition dipole moments known from the absorption spectrum of the BChl. According to the conventional Gouterman model of electronic structure of chlorophyll molecules[39] the strongest transitions are assigned to two Q and two B bands. The latter are often called Soret bands. The two Q transitions are as follows: Q_y at ~12 700 cm^{-1} with a transition dipole moment μ_{Q_y} of 6.3 D and Q_x at ~16500 cm^{-1} and a transition dipole moment μ_{Q_x} of 3.0 D. The two Soret transitions are: B_x at ~25 000 cm^{-1} and μ_{B_x} of 4.6 D; and B_y at ~27 000 cm^{-1} and μ_{B_y} of 6.9 D. The indices *x* and *y* give the transition dipole moment orientation according to the molecular *x* and *y* axes; see Figure 1. The dipole moments of the electronic states are not generally known. For the ground-state we used the calculated electric dipole from He et al.[24] The electric dipole moments of Q_y and Q_x were obtained from the ground-state dipole moment together with the $\Delta\mu_0$ from Table 3. To keep the number of free parameters as low as possible all other dipole moments were set to zero.

The Q_y state is known to have a strong absorption to higher excited states,[40,41] indicating a state (or states) at approximately double the Q_y energy ~26 000 cm^{-1}, with a transition dipole moment oriented 46° with respect to μ_{Q_y}.[40] Energetically the states responsible for that absorption can be due to the Soret bands. Parity selection rules of dipole-allowed transitions would not allow transitions between states which both have strong transition dipole moments from the ground states. For example, in symmetric polyenes and carotenoids, the parity selection rule is known to be well satisfied.[43,44] However, the symmetry of the BChl molecule is not perfect, and it is questionable how well this selection rule holds here. Consequently the state at ~26 000 cm^{-1} can be due to either the Soret bands or to some additional state which do not have absorption from the ground state. We tried both options in our multilevel model. In the first case, we allowed the electronic transition between Q_y and Soret. In the latter case, we introduced a state resonant with B_y, which had zero transition dipole moment from the ground state.

Simulations with only the above states (not shown) did not lead to even qualitative resemblance with TDDFT. It was not possible to reproduce the downward-going trends of transition energies for higher field strengths. It was necessary to introduce additional states coupled to the Q states. Several quantum chemistry calculations of BChl and Chl indicate that there may exist more excited singlet electronic states in the visible spectral region besides the conventional Q and Soret states.[22,42,45,46] Absorption spectrum of the BChl reveals a clear shoulder to the red from the B_x band. We assigned this shoulder to a state which is weakly coupled to the ground state, and estimated the corresponding transition dipole moment from the absorption spectrum in Figure 6. We allowed this state to be coupled to the Q_x state. We are not aware of any experiments reporting the absorption from Q_x to higher excited states. Consequently the possible transition is taken as an adjustable parameter. Besides these states we found it necessary to introduce at least one more state which coupled to both the Q_y and Q_x states. Thus, the minimum multilevel model of BChl capable to describe the TDDFT results is the seven-level system (ground state + six excited states) shown in Figure 3. The two lowest transition energies as a function of the electric field for the seven-level system is shown Figure 6. Here we stress that this is really a minimum model. In general, the more states one introduce the more flexibility one has and the fit becomes better. Naturally there are more high-energy states with possible coupling to ground state and/or Q states.

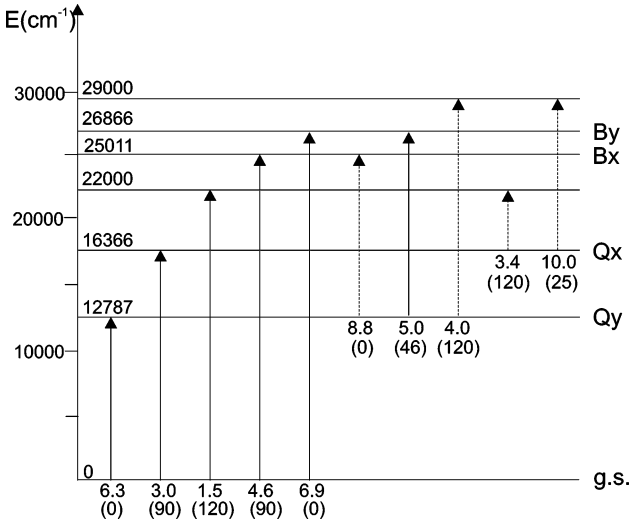

Figure 3. Multilevel model of the BChl energy levels used for the effective Hamiltonian. The transition dipoles in Debye and the direction in the parentheses given in degrees with respect to the gs → Q_y transition dipole moment. Dashed lines represent transitions which have not been established experimentally.

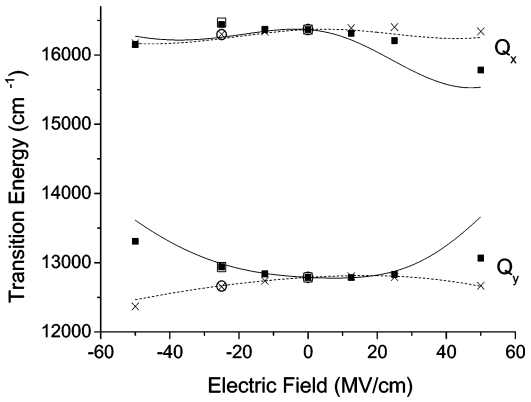

Figure 4. Q_y and Q_x transition energies as a function of the electric field calculated with the Hamiltonian in eq 3. Filled and dashed lines are for the field directions, respectively. TDDFT results are the same as in Figure 2.

When the multilevel system has been established, the transition energies and transition dipole moment for any direction and strength of the field can be calculated. In Figure 6 it is displayed how the transition energies of the Q_y and Q_x state vary as the field is turned 180°. Also shown in Figure 6 is the dependence of the dipole strength of the Q_y transition on field direction and strength.

4. Comparison with Experiments and Discussion

Molecular electrooptical properties $\Delta\alpha$ and $\Delta\mu$ are mainly obtained from three different experimental methods: flash photolysis microwave conductivity,[47] solvent shift measurements of the absorption maxima,[36,37] and Stark spectroscopy.[28−30] The latter two have been applied to BChl molecules.[28,30,49] For a thorough comparative discussion of various experimental results, we refer the interested readers to article.[28] Considerable divergence occurs between results obtained by different methods and different groups; see Table 4. This can be related to the fact that the maximal external fields used in Stark spectroscopy

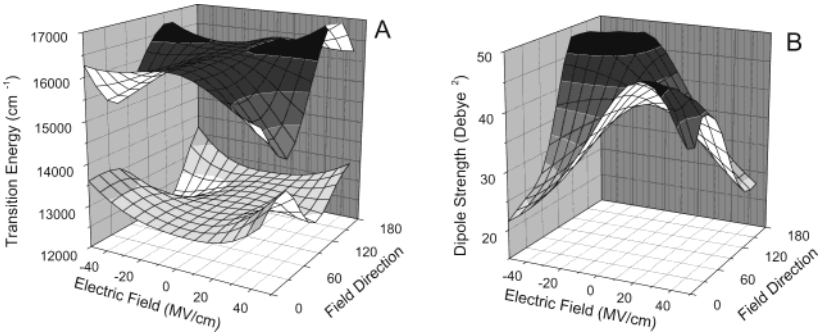

Figure 5. (A) Q_y and Q_x transition energies depending on field direction and strength. (B) Q_y dipole strength for different field directions. The field direction is zero degrees when it is aligned with the gs → Q_y transition dipole moment.

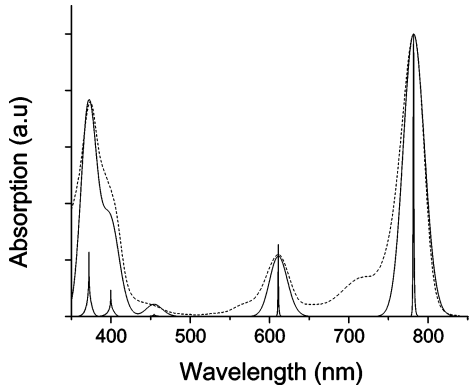

Figure 6. Absorption spectrum from bacteriochlorophyll-*a* in pyridine, absorption maximum at 781.5 nm, with calculated unconvoluted and convoluted spectra. The Gaussians used in the convolution had fwhm of 510 (gs → Q_y), 700 (gs → Q_x), 1000, 1500 (gs → B_x) and 1600 (gs → B_y) cm^{-1}.

TABLE 4: Experimental Results on Polarizability and Dipole Moment Differences

system	$f\Delta\mu$ (D)	$f^2\mathrm{Tr}(\Delta\alpha)$ (Å^3)
Rb. sphaeroides B800 (Q_y)[30]	1.1	5
Rb. sphaeroides B800 (Q_y)[48]	0.8−0.9	
Rb. sphaeroides B800 (Q_y)[28]	0.9 (0.7)[a]	
FMO Cl tepidum B825 (Q_y)[28]	0.51 (0.72)[a]	
BChl in nonpolar solvent		
(Q_y)[49]		16[b]
(Q_x)[49]		13[b]

[a] In parentheses $f\Delta\mu\perp$ where the applied field and the laser polarization are perpendicular. [b] No local filed correction factor f^2.

experiments are usually at least an order of magnitude weaker than the fields induced by the local environment. This makes it difficult to distinguish the molecular $\Delta\mu$ from the $\Delta\mu_{ind}$ originated from matrix-induced change in the electrical dipole due to the $\Delta\alpha$. Weak external fields also mean that the quadratic terms ($\Delta\alpha E^2$) are very small reducing accuracy of the $\Delta\alpha$ estimates. In Table 4, we have collected the most relevant experimental electrooptical parameters of BChl known to us. Comparing the experimental $Q_y\Delta\mu$ with our fitting results in Table 3, we notice that the experimental values are considerably larger. Also the calculations of $\Delta\mu$ with B800 where the local environment was partly taken into account has given substantially higher values.[24] This discrepancy is mainly due to the $\Delta\mu_{ind}$. After adjusting the results of the Stark holeburning measurements to the $\Delta\mu_{ind}$, Rätsep et al.[28] concluded that the molecular $\Delta\mu$ can be as low as 0.2 D. The Lorentz isotropic local field correction $f = (\epsilon + 2)/3$ with a static dielectric constant epsilon of about 2 is often used for photosynthetic complexes. This leads to a $\Delta\mu$ very close to what our current calculations yield. It is noteworthy that fitting of the TDDFT results to eq 2 give us a negative $\Delta\alpha_{yy}$. Also the orientationally averaged polarizability difference $^1/_3\mathrm{Tr}(\Delta\alpha)$ is negative. No experiment has so far suggested $\Delta\alpha < 0$ for that transition. The typical external field strengths used in above Stark spectroscopy experiments is around 0.1 MV/cm. Such a field shifts the absorption spectrum of a molecule with $\Delta\alpha = 10$ Å by less than 0.01 cm^{-1}, whereas the broadening of the line due to the $\Delta\mu = 1$ D is more than 2 orders of magnitude larger. It is unlikely that such a small shift accompanied by a strong broadening could have been detected. Solvatochromic shift estimates of the $\Delta\alpha$[49] are based on the Bakhshiev equation[50] which is essentially the London approximation.[51] To derive the Bakhshiev equation one needs to make assumptions (average energy approximation, e.g.) which are not always justified.[52] Particularly for the excited states the dispersion interaction expression contains elements where the energy difference has opposite signs breaking down the average energy approximation. We have numerically verified that the multilevel molecule what we have used to simulate the TDDFT calculations still leads to the red-shift of the Q_y transition with increasing solvent polarizability even though the $\Delta\alpha < 0$. It will be interesting to see whether our prediction of the negative polarizability change of the Q_y transition in BChl will be supported by the future more precise experiments.

Low-temperature spectra of BChl in solution or in protein are inhomogeneously broadened.[25,26] Part of the inhomogeneous broadening can be seen as a result of an inhomogeneous local field of the BChl. Following the procedure for simulating the absorption spectra as described by ref 27 and adding orientational averaging over the field direction, we have calculated an electric field broadened BChl spectrum. The field was in the *XY* plane and the strength had a Gaussian distribution with a fwhm of 10 MV/cm. The spectrum is shown in Figure 6. To account for other broadening mechanisms (dispersion interaction, electron−phonon interaction, etc.) the narrow lines from the field-broadening calculations were convoluted with Gaussians of different widths.

5. Conclusion

TDDFT calculations of a BChl molecule in electric field have enabled us to obtain detailed information about electrochromic properties of the Q_y and Q_x transitions. Most remarkably, we found that $\Delta\alpha_{yy}$ is negative. Even average $\Delta\alpha$ is negative for the Q_y. A minimum multilevel model of a molecule, capable of describing the electric field effects, was constructed.

It was found that to reach agreement with TDDFT calculations of the system it was necessary to introduce additional states besides the conventional Q and Soret bands.

Acknowledgment. We thank Dr. T. Polivka for stimulating discussions. This work was supported by the Swedish Research Council. Calculations were partially carried out using facilities of the National Supercomputer Center (NSC) in Linköping, Sweden.

References and Notes

(1) van Grondelle, R. *Biochim. Biophys. Acta* **1985**, *811*, 147.
(2) van Grondelle, R.; Dekker: J. P.; Gillbro, T.; Sundström, V. *Biochim. Biophys. Acta* **1994**, *1187*, 1.
(3) Pullerits, T.; Sundström, V. *Acc. Chem. Res.* **1996**, *29*, 381.
(4) Fleming, G. R.; van Grondelle, R. *Curr. Opin. Struct. Biol.* **1997**, *7*, 738.
(5) Sundström, V.; Pullerits, T.; van Grondelle, R. *J. Phys. Chem. B* **1999**, *103*, 2327.
(6) McDermott, G.; Prince, S. M.; Freer, A. A.; Hawthornthwaite-Lawless, A. M.; Papiz, M. Z.; Cogdell, R. J.; Isaacs, N. W. *Nature (London)* **1995**, *374*, 517.
(7) Koepke, J.; Hu, X.; Muenke, C.; Schulten, K.; Michel, H. *Structure* **1996**, *4*, 581.
(8) Louwe, R. J. W.; Vrieze, J.; Hoff, A. J.; Aartsma, T. J. *J. Phys. Chem. B.* **1997**, *101*, 11280.
(9) Pullerits, T.; Chachisvilis, M.; Sundström, V. *J. Phys. Chem.* **1996**, *100*, 10787.
(10) Monshouwer, R.; Abrahamsson, M.; van Mourik, F.; van Grondelle, R. *J. Phys. Chem. B* **1997**, *101*, 7241.
(11) Sauer, K.; Cogdell, R. J.; Prince, S. M.; Freer, A. A.; Isaacs, N. W.; Scheer, H. *Photochem. Photobiol.* **1996**, *64*, 564.
(12) Alden, R. G.; Johnson, E.; Nagarjan, V.; Parson, W. W.; Law, C. J.; Cogdell, O. J. G. *J. Phys. Chem. B* **1997**, *101*, 4667.
(13) Hu, X.; Ritz, T.; Damjanovic, A.; Schulten, K. J. *J. Phys. Chem. B* **1997**, *101*, 3854.
(14) Dracheva, T. V.; Novoderezhkin, V. I.; Razjivin, A. P. *FEBS Lett.* **1996**, *387*, 81.
(15) Scholes, G. D.; Gould, I. R.; Cogdell, R. J.; Fleming, G. R. *J. Phys. Chem. B* **1999**, *103*, 2543.
(16) Parson, W. W.; Warshel, A. *J. Am. Chem. Soc.* **1987**, *109*, 6152.
(17) Gudowska-Nowak, E.; Newton, M. D.; Fajer, J. *J. Phys. Chem.* **1990**, *94*, 5795.
(18) Fowler, G. J. S.; Visschers, R. W.; Grief, G. G.; van Grondelle, R.; Hunter, C. N. *Nature (London)* **1992**, *355*, 848.
(19) Hess, S.; Visscher, K. J.; Pullerits, T.; Sundström, V.; Fowler, G. J. S.; Hunter, C. N. *Biochemistry* **1994**, *33*, 8300.
(20) Fowler, G. J. S.; Hess, S.; Pullerits, T.; Sundström, V.; Hunter, C. N. *Biochemistry* **1997**, *36*, 11282.
(21) He, Z.; Pullerits, T. Unpublished work.
(22) He, Z.; Sundström, V.; Pullerits, T. *J. Phys. Chem. B* **2002**, *106*, 11606.
(23) Herek, J. L.; Polivka, T.; Pullerits, T.; Fowler, G. J. S.; Hunter, C. N.; Sundström, V. *Biochemistry* **1998**, *37*, 7057.
(24) He, Z.; Sundström, V.; Pullerits, T. *Chem. Phys. Lett.* **2001**, *334*, 159.
(25) Pullerits, T.; Visscher, K. J.; Hess, S.; Sundström, V.; Freiberg, A.; Timpmann, K.; van Grondelle, R. *Biophys. J.* **1994**, *66*, 236.
(26) Ormos, P.; Ansari, A.; Braunstein, D.; Cowen, B. R.; Frauenfelder, H.; Hong, M. K.; Iben, I. E. T.; Sauke, T. B.; Steinbach, P. J.; Young, R. D. *Biophys. J.* **1990**, *57*, 191.
(27) van Mourik, F.; van der Zwan, G.; Chergui, M. *J. Phys. Chem. B* **2001**, *105*, 9715.
(28) Rätsep, M.; Wu, H.-M.; Hayes, J. M.; Blankenship, R. E.; Cogdell, R. J.; Small, G. J. *J. Phys. Chem. B* **1998**, *102*, 4035.
(29) Lockhart, D. J.; Boxer, S. G. *Proc. Natl. Acad. Sci. U.S.A* **1988**, *85*, 107.
(30) Beekman, L. M. P.; Freese, R. N.; Fowler, G. J. S.; Picorel, R.; Cogdell, R. J.; van Stokkum, I. H. M.; Hunter, C. N.; van Grondelle, R. *J. Phys. Chem. B* **1997**, *101*, 7293.
(31) Grozema, F. C.; Telesca, R.; Jonkman, H. T.; Siebbeles, L. D. A.; Snijders, J. G. *J. Chem. Phys.* **2001**, *115*, 10014.
(32) Becke, A. D. *J. Chem. Phys.* **1993**, *98*, 5648.
(33) Frisch, M. J.; Trucks, G. W.; Schlegel, H. B.; Scuseria, G. E.; Robb, M. A.; Cheeseman, J. R.; Zakrzewski, V. G.; Montgomery, J. A., Jr.; Stratmann, R. E.; Burant, J. C.; Dapprich, S.; Millam, J. M.; Daniels, A. D.; Kudin, K. N.; Strain, M. C.; Farkas, O.; Tomasi, J.; Barone, V.; Cossi, M.; Cammi, R.; Mennucci, B.; Pomelli, C.; Adamo, C.; Clifford, S.; Ochterski, J.; Petersson, G. A.; Ayala, P. Y.; Cui, Q.; Morokuma, K.; Malick, D. K.; Rabuck, A. D.; Raghavachari, K.; Foresman, J. B.; Cioslowski, J.; Ortiz, J. V.; Stefanov, B. B.; Liu, G.; Liashenko, A.; Piskorz, P.; Komaromi, I.; Gomperts, R.; Martin, R. L.; Fox, D. J.; Keith, T.; Al-Laham, M. A.; Peng, C. Y.; Nanayakkara, A.; Gonzalez, C.; Challacombe, M.; Gill, P. M. W.; Johnson, B.; Chen, W.; Wong, M. W.; Andres, J. L.; Gonzalez, C.; Head-Gordon, M.; Replogle, E. S.; Pople, J. A. *Gaussian 98*; Carnegie-Mellon University: Pittsburgh, PA, 1998
(34) Hartwich, G.; Fiedor, L.; Simonin, I.; Cmiel, E.; Schafer, W.; Noy, D.; Scherz, A.; Scheer, H. *J. Am. Chem. Soc.* **1998**, *120*, 3675.
(35) Pullerits, T.; Hess, S.; Herek, J. L.; Sundström, V. *J. Phys. Chem.* **1997**, *101*, 10560.
(36) Renge, I. *Chem. Phys.* **1992**, *167*, 173.
(37) Limantara, L.; Sakamoto, S.; Koyama, Y.; Nagae, H. *Photochem. Photobiol.* **1997**, *65*, 330.
(38) Petke, J.; Maggiora, G. M. *J. Chem. Phys.* **1986**, *84*, 1640.
(39) Gouterman, M. *J. Mol. Spectrosc.* **1961**, *6*, 138.
(40) Martinsson, P.; Sundström, V.; Åkesson, E. *FEBS Lett.* **2000**, *465*, 107.
(41) Becker, M.; Nagarajan, V.; Parson, W. W. *J. Am. Chem. Soc.* **1991**, *113*, 6840.
(42) Parusel, A. B. J.; Grimme, S. *J. Phys. Chem. B* **2000**, *104*, 5395.
(43) Schulten, K.; Karplus, M. *Chem. Phys. Lett.* **1972**, *14*, 305.
(44) Tavan, P.; Schulten, K. *Phys. Rev. B* **1987**, *36*, 4337.
(45) Hsu, C.-P.; Walla, P. J.; Head-Gordon, M.; Fleming, G. R. *J. Phys. Chem. B* **2001**, *105*, 11016.
(46) Sundholm, D. *Chem. Phys. Lett.* **1999**, *302*, 480.
(47) Gelnick, G. H.; Piet, J. J.; Wegewijs, B. R.; Müllen, K.; Wilderman, J.; Hadiziioannou, G.; Warman, J. M. *Phys. Rev. B* **2000**, *62*, 1489.
(48) Gottfried, D. S.; Stocker, J. W.; Boxer, S. G. *Biochim. Biophys. Acta* **1991**, *1059*, 63.
(49) Renge, I. *J. Phys. Chem.* **1993**, *97*, 6582.
(50) Renge, I.; Mölder, U.; Koppel, I. *Spectrochim. Acta* **1985**, *41A*, 967.
(51) London, F. *Trans. Faraday. Soc.* **1937**, *33*, 8.
(52) Amos, A. T.; Burrows, B. L. *Adv. Quantum Chem.* **1973**, *7*, 289.